

Specific Degradation of the Mucin Domain of Lubricin in Synovial Fluid Impairs Cartilage Lubrication

Megh Prajapati, Karan Vishwanath, Lingting Huang, Marshall Colville, Heidi Reesink, Matthew Paszek, and Lawrence J. Bonassar*



Cite This: *ACS Biomater. Sci. Eng.* 2024, 10, 6915–6926



Read Online

ACCESS |

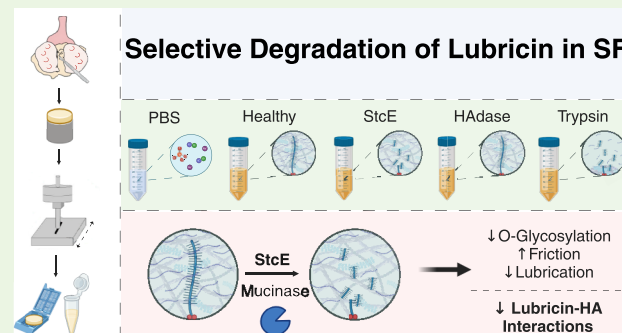
Metrics & More

Article Recommendations

Supporting Information

ABSTRACT: Progressive cartilage degradation, synovial inflammation, and joint lubrication dysfunction are key markers of osteoarthritis. The composition of synovial fluid (SF) is altered in OA, with changes to both hyaluronic acid and lubricin, the primary lubricating molecules in SF. Lubricin's distinct bottlebrush mucin domain has been speculated to contribute to its lubricating ability, but the relationship between its structure and mechanical function in SF is not well understood. Here, we demonstrate the application of a novel mucinase (StcE) to selectively degrade lubricin's mucin domain in SF to measure its impact on joint lubrication and friction. Notably, StcE effectively degraded the lubricating ability of SF in a dose-dependent manner starting at nanogram concentrations (1–3.2 ng/mL). Further, the highest StcE doses effectively degraded lubrication to levels on par with trypsin, suggesting that cleavage at the mucin domain of lubricin is sufficient to completely inhibit the lubrication mechanism of the collective protein component in SF. These findings demonstrate the value of mucin-specific experimental approaches to characterize the lubricating properties of SF and reveal key trends in joint lubrication that help us better understand cartilage function in lubrication-deficient joints.

KEYWORDS: PRG 4, cartilage, joint fluid, glycosylation, tribology



INTRODUCTION

Osteoarthritis (OA) is a degenerative joint disease characterized by progressive cartilage degradation, synovial inflammation, and alterations in joint lubrication.^{1–3} Synovial fluid (SF) is a viscous non-Newtonian fluid that is present in the joint space and plays a critical mechanical role in maintaining joint health by reducing friction and minimizing direct contact between articulating surfaces during joint motion.^{4–7} In OA, changes in SF composition and properties are implicated in joint dysfunction following inflammation or injury, leading to a loss of lubrication and further progression of the disease.^{8–11} Similarly, articular cartilage provides mechanical support, load bearing, and lubrication.^{12,13} Cartilage matrix degradation in osteoarthritic joints is also associated with high friction conditions, in which increased coefficients of friction correlate to increased wear and tear, with implications to poor clinical outcomes.^{1,14–16}

At the molecular level, the remarkable low friction properties of healthy cartilage are thought to be attributed to the synergistic interactions between two macromolecules in the SF: hyaluronic acid (HA), a viscous anionic nonsulfated glycosaminoglycan, and lubricin (proteoglycan 4, PRG4), a mucinous glycoprotein with a bottlebrush structure that enhances localization of HA to the surface of the tissue.^{17–21}

Lubricin's mucin domain, flanked by Somatomedin B-like and hemopexin-like domains, is thought to confer distinct molecular and chemical properties to the molecule like the ability to hydrate, lubricate, and shield biological interfaces.^{22–24} Previous work has shown that lubricin's ability to act as a boundary lubricant is attributed to the O-linked oligosaccharide side chains that enable molecular entanglement of HA, leading to a gel-like layer at the articulating surface that provides hydration and possibly greater local viscosities.^{22,25} In healthy joints, the synergistic interplay of these two macromolecules in the SF reduces the coefficient of friction and promotes a transition to low friction environments, consistent with the tribological theory of viscous boundary lubrication.^{20,25,26} Conversely, in osteoarthritic joints, these same macromolecular interactions are disrupted, in large part due to reduced or altered lubricin concentrations in SF as

Received: May 17, 2024

Revised: October 7, 2024

Accepted: October 8, 2024

Published: October 19, 2024



previous studies have reported.^{27,28} Therefore, understanding lubricin function directly informs OA pathophysiology.

The critical role of the collective protein content of SF in lubrication has been shown in multiple studies using nonspecific proteases such as trypsin.^{25,29–33} While these studies provide valuable insight into SF protein function, the lack of specificity of these enzymes makes it difficult to determine the exact molecular mechanisms involved. Further, the high density of branches in lubricin's mucin domain makes it resistant to digestion by conventional proteases like trypsin, leaving much of the domain of interest unanalyzed.^{34,35} As such, due to constraints in glycosylation and protease resistance, the selective degradation of the mucin domain in lubricin has not been possible to date.³⁶ This leaves a critical gap in our ability to probe structure–function relationships in cartilage lubrication.

However, recent advancements in glycobiology and recombinant biosynthesis have spurred focused attempts at understanding aberrant mucin domain expression patterns in diseased pathologies. While previous studies have specifically targeted glycosylated branches in lubricin by enzymatic removal via glycosidases in latex-on-glass systems, the tribological characterization of synovial fluid in cartilage lubrication with specific truncation of the mucin domain in lubricin has not been possible.²² Recently, a novel recombinant secreted protease of C1 esterase inhibitor (StcE) from enterohemorrhagic *E. coli* was shown to selectively cleave core proteins at their mucin domains.^{35,37} StcE specifically targets mucinous glycoproteins like lubricin and does not affect nonmucin proteins (even if glycosylated) such as hyaluronic acid (HA) or fibronectin.³⁵ Additionally, StcE does not cleave mucins that have been enzymatically deglycosylated. Its unique selectivity to a singular O-GalNAc residue, regardless of the high density or size of attached glycan structures enables its function across a general range of O-glycan modifications. This ability extends to lubricin, allowing StcE to selectively cleave the densely O-glycosylated mucin domain in lubricin from native environments without altering HA composition or structure.³⁸ While the ability of StcE to selectively target lubricin has been characterized in terms of adhesive properties at the ocular interface for mucin deficiency in Dry Eye Disease,³⁹ its specific implications in understanding OA mechanisms and the lubricating environment in SF is not fully understood. Thus, the application of this novel tool in the study of OA and lubricin enables us to bridge the gap in understanding how the mucin domain alters tribological behavior.

With this knowledge gap in mind, the goal of this study was to assess the effect of the StcE mucinase on the tribological properties of SF using the Stribeck framework previously shown to reliably describe cartilage lubrication across all modes and compare these effects to the nonspecific bulk degradation of the protein and HA component of SF by trypsin and hyaluronidase, respectively.^{24,40–44} Further, we compare the biochemical and viscoelastic properties of SF treated with various doses of StcE across several orders of magnitude of physiological articulation speeds to validate its ability to probe the removal of O-linked oligosaccharides of lubricin in SF. We hypothesized that StcE treatment of SF would inhibit its lubricating ability and increase coefficients of friction in a dose-dependent manner without altering the surface properties of the cartilage or the bulk rheology of SF. These results offer new insight into the molecular mechanisms of lubrication in SF and

accordingly aid the development of biomimetic therapeutics that help treat the disease by enhancing our understanding of the specific structural and functional components of lubricin that contribute to SF lubrication.

MATERIALS AND METHODS

2.1. Study Design. To assess the ability and potential of StcE to inhibit SF-mediated cartilage lubrication, we compared StcE-treated bovine synovial fluid (BSF) to established methods of degrading BSF using trypsin and hyaluronidase, which have been previously shown to reliably disrupt the lubricating ability of SF. Further, to analyze the dose-dependent behavior of StcE treatment, variable concentrations of StcE were added to healthy BSF for further frictional characterization. Frictional behaviors were compared in parallel with biochemical compositions to ensure and validate the selectivity of the enzyme.

2.2. Standard Lubricant Treatments. To nonspecifically degrade the protein component of SF, healthy BSF was digested with 50 µg/mL L-1-tosylamido-2-phenylethyl chloromethyl treated trypsin (Sigma-Aldrich) from bovine pancreas for 2 h at 37 °C under constant stirring conditions as previously described.²⁵ To selectively degrade the HA component of synovial fluid, healthy BSF was digested with 25 µg/mL hyaluronidase (Sigma-Aldrich) from bovine testes for 2 h at 37 °C as previously described.²⁵ Phosphate buffered saline (PBS; Corning) and untreated healthy BSF were used as benchmarks for high and low friction, respectively.

2.3. StcE Mucinase Purification. A concentrated 13.7 mg/mL StcE stock solution was prepared via a previously described combination of gene synthesis and assay purification. Briefly, the cDNA encoding StcE-Δ35 was prepared and integrated into an expression vector. StcE-expressing cells were harvested by centrifugation at 3000g for 20 min and lysed in a buffer containing HEPES, NaCl and imidazole supplemented with a protease inhibitor cocktail. The enzyme was subsequently purified by immobilized metal affinity chromatography (IMAC), imidazole gradient elution, size-exclusion chromatography and further concentrated with a 30 kDa molecular weight filter culminating in the final stock solution.

2.4. StcE Lubricant Treatments. The effect of StcE treatment on SF lubrication was analyzed in 11 different StcE doses across 4 orders of magnitude. Briefly, the 13.7 mg/mL StcE solution was serially diluted in half-log increments to obtain concentrations ranging from 10 µg/mL to 0.32 ng/mL of StcE in BSF. Each StcE treated sample was incubated at 37 °C for 2 h under constant stirring conditions. All treated samples were stored at –20 °C for 24 h and thawed for 15 min in a water bath at 37 °C prior to friction testing.

2.5. Friction Characterization of StcE Treated BSF. Frictional characterization of all the lubricant samples was performed using a previously described, custom cartilage-on-glass tribometer system.^{25,41,45,46} Briefly, cylindrical cartilage explants (6 mm diameter) obtained from the femoral condyles of neonatal bovine stifles were trimmed to a height of 2 mm and slid against a polished glass surface while bathed in lubricating baths of PBS, healthy BSF or enzymatically treated BSF. Explants ($n = 5$ per treatment group for 13 SF conditions) were compressed to a 30% strain via a custom compound screw that allowed for translation of the load cell in the normal direction and subsequent application of normal strain to the tissue. Samples were allowed to stress relax for 1 h to mitigate the effects of interstitial fluid pressurization and evaluate the coefficient of friction under conditions of boundary lubrication. Following equilibration with ambient pressure, the glass counterpart was linearly reciprocated at predetermined sliding speeds ranging from 0.1 to 10 mm/s for ~2.75 h. These compression strain levels and sliding speeds were chosen based on strong correlations of this system's friction data to improvements in patient WOMAC scores.⁴⁷ The coefficient of friction (μ) was recorded as the ratio of the shear to the normal load as calculated from the transformation of shear and normal voltages obtained by a biaxial load cell. To counteract the boundary lubrication effects of directional changes in sliding, shear load data was manually processed to eliminate data points where the linearly reciprocating

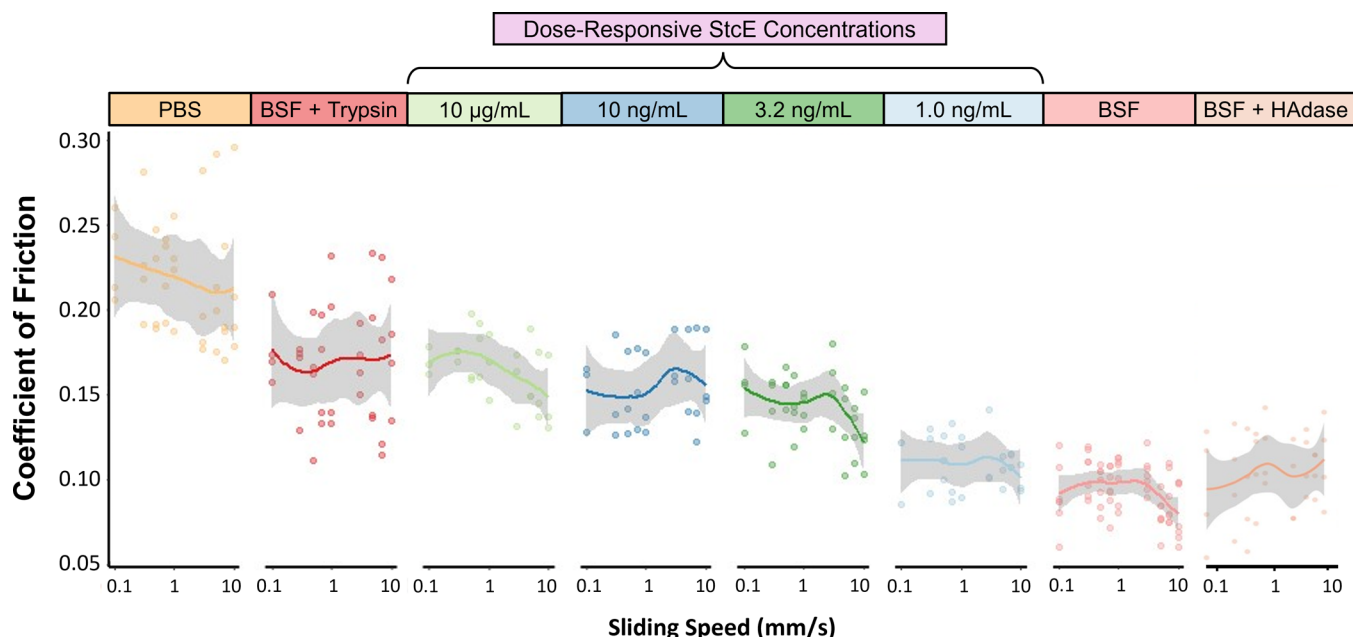


Figure 1. Coefficient of friction for various doses of StcE across 3 orders of magnitude of articulation speed ($n = 3\text{--}5$ per concentration per speed) reveals the dose-dependent effect of StcE on SF lubrication. The significant change in friction of the trypsin treated BSF compared to the HAdase treated BSF verifies that synovial fluid's protein component contributes significantly to its low friction properties. The shaded gray area represents the 95% confidence interval for the linear regression model.

platform reversed direction.⁴¹ All coefficients were calculated at the end of sliding when friction reached an equilibrium value and was averaged in both directions to obtain a mean value for friction at each sliding speed.⁴⁸

2.6. Histology. Immediately after friction testing, explants were fixed in 10% phosphate-buffered formalin for 3 to 5 days, and then transferred to 70% ethanol for histological processing. Samples were embedded in paraffin wax, sectioned to 5 μm , mounted on clear glass slides, and stained with Safranin-O to observe changes in proteoglycan or glycosaminoglycan (GAG) content. Samples from healthy BSF and StcE-treated BSF were analyzed and imaged via brightfield microscopy to determine effects of StcE on cartilage integrity.

2.7. Rheology. Immediately after friction testing, synovial fluid was recovered. To determine whether StcE altered the viscosity of synovial fluid, a commercial rheometer (TA Instruments DHR3 Rheometer, New Castle, DE) was used to measure the shear rate-dependent viscosity of healthy BSF and the highest dose of StcE-treated BSF (10 $\mu\text{g/mL}$).⁴⁹ A 40 mm diameter cone-and-plate fixture with a 2-degree angle was used to perform a shear rate sweep of $\dot{\gamma} = 0.01$ to 1.0 s^{-1} on all doses of StcE and determine the dynamic viscosities based on protocols built into the Trios software.

2.8. Western Blots. Western Blots were used for immunodetection of lubricin in recovered SF samples that were treated with StcE. An antilubricin monoclonal antibody 9G3 from Sigma (MABT401) was used.⁵⁰ Briefly, SF samples were transferred to nitrocellulose membranes at 15 V overnight and blocked for 30 min in 5% w/v Normal Goat Serum (NGS) and TBST (20 mM Tris and 150 mM NaC, PH 7.5 with 0.01% w/v Tween 20). Sample membranes were incubated with the monoclonal antibody 9G3 (1:1000 dilution in TBST) for 1 h at 4 °C, incubated with Anti-Mouse DyLight 800 secondary antibodies (1:5000 dilution in TBST), and analyzed for immunoreactive bands using a Western Blotting detection kit with a three-step wash cycle in TBST (TBS with 0.01% w/v Tween 20) before and after each incubation step.⁵⁰ Protein samples were denatured by mixing with NuPAGE LDS sample buffer (Invitrogen) and NuPAGE sample reducing agent (Invitrogen) and heated at 95 °C for 10 min. The denatured protein samples were separated on NuPAGE 3–8% Tris-acetate gels (Invitrogen) according to manufacturer's instructions and subsequently stained with Pierce

silver stain kit (Thermo Scientific) or transferred to nitrocellulose (Thermo Scientific) membranes according to manufacturer's protocols.

2.9. Statistical Analysis. A linear mixed effects regression model was used to fit coefficient of friction as a function of sliding speed, lubricant type, and StcE concentration. Random effects in the model include the sliding speed order, treatment number based on date of test, and joint from which cartilage explants were obtained. A 4-parameter variable slope concentration response (VSCR) model was fitted to the friction-StcE concentration data to obtain the ED_{50} for StcE and the minimum dose of StcE needed to disrupt the lubricating ability of BSF (eq 1) where A and B were defined as the high and low friction plateaus, respectively.⁴¹

$$\mu = B + \frac{A - B}{1 + \left(\frac{ED_{50}}{[StcE]} \right)^d} \quad (1)$$

Posthoc pairwise comparisons were conducted to estimate statistical differences in the marginal means of the friction coefficient and ED_{50} at each speed and StcE concentration. Significance was evaluated at $p < 0.05$. All statistical analyses were performed in MATLAB and RStudio. The Stribeck surface was generated by interpolating the friction data to logarithmically spaced vectors that correspond to concentration and articulation speed coordinate ranges. Triangulation-based natural neighbor interpolation enabled for an efficient trade-off between linear and cubic interpolation, accounting for associated variation.

RESULTS

Tribology of General Protein and HA Contributions to SF Lubrication. To assess the relative contributions of HA and protein to SF lubrication, we compared the coefficients of friction for PBS, trypsin-treated BSF, hyaluronidase-treated BSF, and healthy BSF (Figure 1). While neither of the two enzyme treatments completely inhibited SF lubrication, the combined effects of trypsin ($\Delta\mu = 0.06\text{--}0.07$) and hyaluronidase (HAdase, $\Delta\mu = 0.02\text{--}0.03$) largely accounted for the friction difference between BSF and PBS ($\Delta\mu = 0.10\text{--}0.12$). As

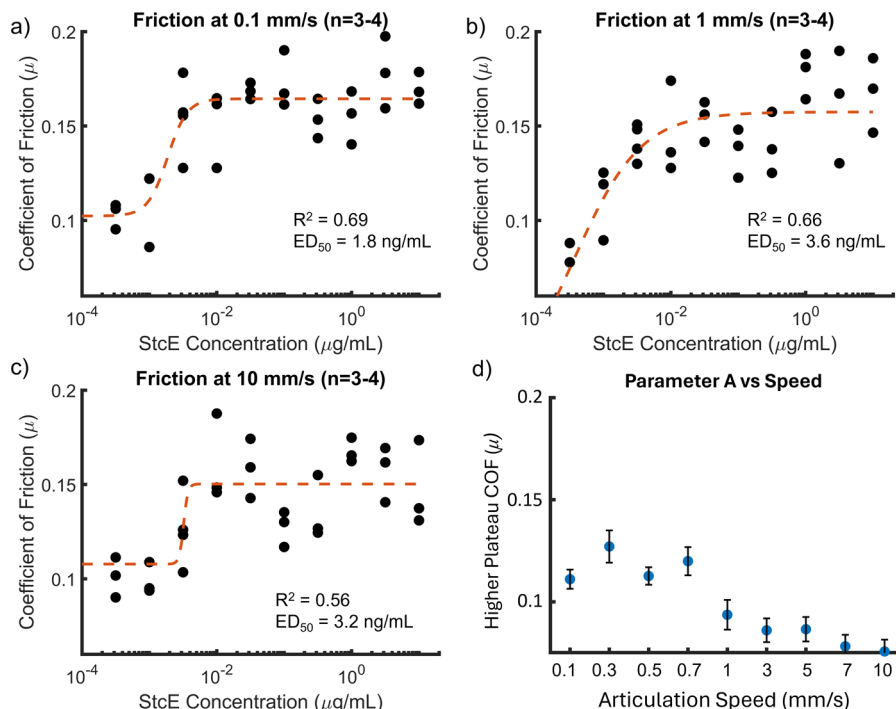


Figure 2. Four parameter Dose-response Models for friction as a function of StcE concentration at sliding speeds across 3 orders of magnitude at 0.1 mm/s (A), 1 mm/s (B), 10 mm/s (C) for $n = 3–5$ per concentration per speed confirms dose-dependent behavior of StcE degradation. Note that the data points in black represent the averages of experimentally obtained data. The fit parameter A (the upper plateau for friction coefficient) decreases with increasing articulation speed (D).

expected, PBS-lubricated explants showed significantly higher coefficients of friction compared to healthy BSF across the entire range of sliding speeds ($p < 0.001$, Figure 1) at $\mu_{\text{avg}} = 0.22$, a number in agreement with previously reported data for this system.²⁵ Similarly, coefficients of friction for healthy BSF ($\mu = 0.06–0.11$) were consistent with previous literature for healthy BSF measured on this system.²⁵ Additionally, there was a significant difference in the coefficient of friction between the trypsin-treated BSF ($\mu = 0.17$) and all other BSF groups ($p < 0.05$), indicating that the protein content of SF was a major contributor to joint lubrication as reported previously.^{29,51} While the BSF + HAdase treatment group had higher coefficients than the healthy BSF group, these differences were not significant ($p > 0.05$).

Tribology of Lubricin-Specific Contributions to SF Lubrication. StcE altered the lubricating ability of SF in a dose-dependent manner, with increasing concentrations of StcE in BSF leading to increased coefficients of friction (Figure 1). Lower concentrations of StcE (under 0.32 ng/mL) had no effect on the lubricating ability of BSF with $\mu_{\text{avg}} = 0.09$ revealing no differences from the healthy BSF group ($p > 0.05$). The minimal effective concentration of StcE was found to be between 1 and 3.2 ng/mL. With each increasing dose, friction increased significantly between 1.0 ng/mL and 10 ng/mL ($p < 0.05$ between all effective doses). The maximum effective concentration of StcE was found to be 10 ng/mL. For all tested concentrations greater than 10 ng/mL up to the highest assessed dose at 10 μg/mL, friction values plateaued and showed no differences between doses ($\mu = 0.17$, $p > 0.05$).

Dose-Dependence of StcE Treatment. Analysis using a 4-parameter VSCR Model confirmed that StcE exhibited a dose-dependent relationship with friction across all articulation speeds ($p < 0.01$) (Figure 2). The lubrication treatments were

fit to Equation 1 with adjusted R^2 values ranging from 0.56 to 0.92 across all speeds. Curve fits revealed ED_{50} values ranging from 1.6 to 3.6 ng/mL depending on the articulation speed (Figure 2A-C). While there was no significant trend between ED_{50} and articulation speed, the high dose plateau for the coefficient of friction (parameter A in eq 1) decreased with increasing articulation speed (Figure 2D) ($p < 0.05$).

Speed Dependence and Lubrication Mode Transition across StcE Doses. The Stribeck surface for StcE treatment across doses revealed a shift in friction ranging between values observed for healthy BSF (lower blue plane, $\mu = 0.09$) and trypsin-treated BSF (yellow plane, $\mu = 0.17$) across different speed regimes and doses (Figure 3). Lubrication was not disrupted to the extent of PBS levels (upper red plane, $\mu = 0.22$). At low speeds and high StcE doses, the increase in friction plateaued, resembling a surface that matched trypsin treatments (yellow plane, $\mu = 0.17$). At high speeds and low StcE doses, the friction surface resembled healthy BSF. Strikingly, at intermediate doses near the ED_{50} , the friction regime most strongly depended on speed, ranging across a large portion of the friction regime (Figure 3). The Stribeck surface analysis revealed that the degradation of lubricin in SF lead to a lubrication mode transition from boundary mode to minimum friction mode, particularly at higher articulation speeds (Figure 3).

Histological Analysis. To investigate changes to the cartilage surface following submersion in the lubricant bath for friction testing, samples were stained in Safranin-O and observed for differences in cartilage structure, integrity, and composition. Safranin-O-stained histological sections of the control samples from healthy BSF were consistent with previously reported data, revealing minimal proteoglycan loss or changes in tissue roughness (Figure 4A).⁴⁵ Further, results

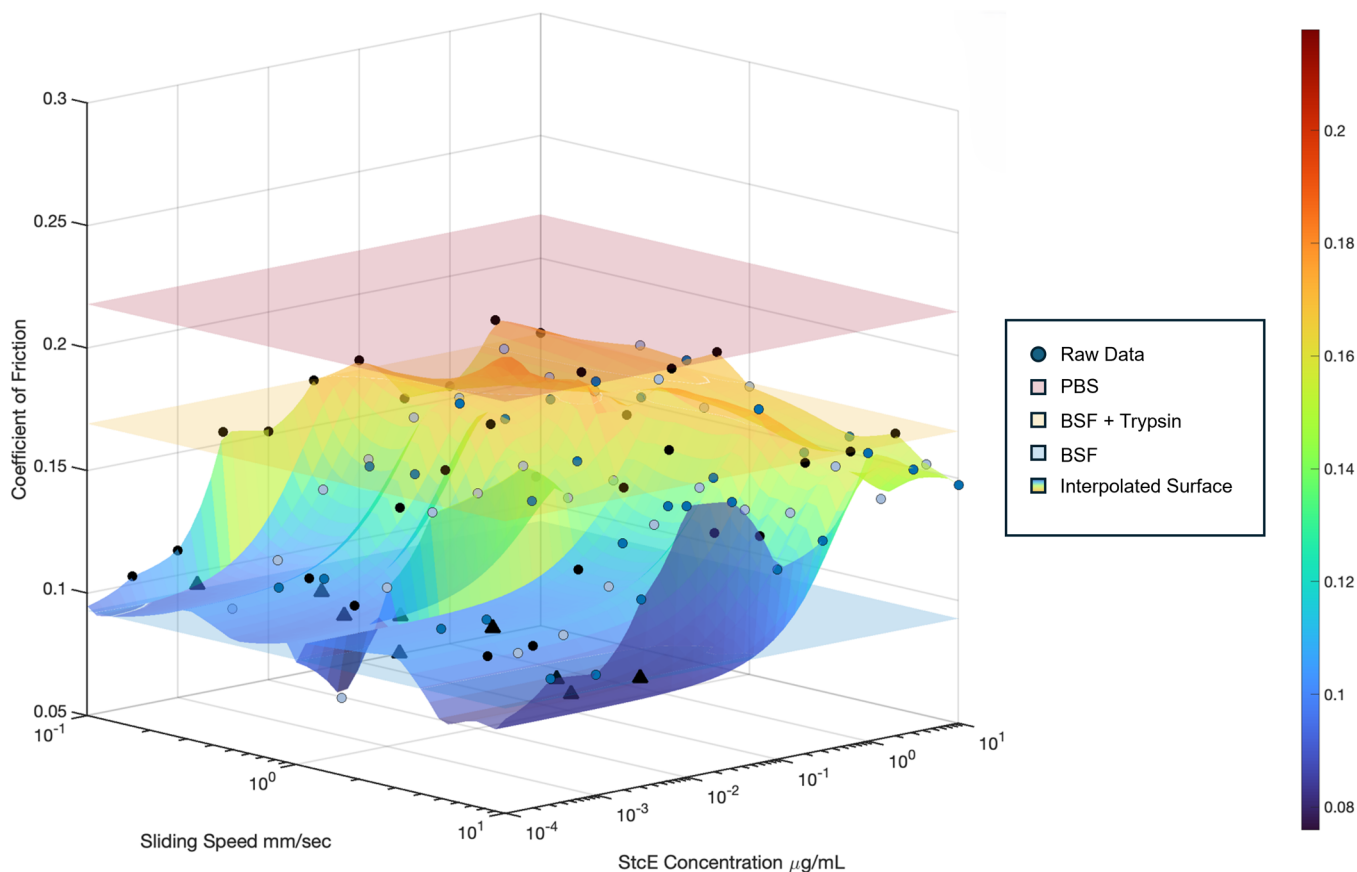


Figure 3. Surface plot of friction as a function of sliding speed and StcE concentration compared to mean friction for PBS, BSF and BSF treated with trypsin reveals elastoviscous transition from boundary mode (high friction) to minimum mode (low friction). The extent of the transition is dependent on articulation speed. Dashed contour line depicts the influence of sliding speed on the ED_{50} concentration at which point speed-dependence is greatest.

showed that cartilage treatment of StcE-treated BSF did not significantly decrease proteoglycan content or alter cartilage surface structure. Histological sections of BSF at the maximum dose and the minimum dose (representative of samples across all 11 doses for $n = 33$) exhibited similar properties, similar to healthy tissue with little to no loss in GAG content (Figure 4B–C). Contrastingly, samples in trypsin treated BSF showed substantially higher surface damage and proteoglycan loss, visible as an absence of Safranin staining the superficial-to-mid zone layers (Figure 4D). This is consistent with previous findings following tribological evaluation.⁵²

Rheological Properties of StcE Treated BSF. To determine whether viscosity of the SF was altered by the presence of StcE, solutions of healthy BSF and BSF treated with 10 $\mu\text{g}/\text{mL}$ of StcE were tested on a rheometer in the cone-and-plate configuration. The dynamic viscosity of the BSF and BSF+StcE across 5 orders of magnitude of shear rate ranged from 0.01–1.00 Pa•s (Figure 5). There were no statistically significant differences in the measured viscosity of healthy and StcE treated BSF, confirming the constant-viscosity assumption model in comparing friction while supporting the validity of StcE as a lubricin-specific enzyme, consistent with previous studies showing minimal contribution of lubricin to SF viscosity in conditions where tertiary and quaternary lubricin interactions are inhibited by disruption of disulfide bonds.^{7,53–55}

Immunodetection of Lubricin in Recovered SF Samples. The expected signal for the 9G3 primary antibody

is present in healthy BSF (Figure 6) and the lowest StcE concentrations. The signal begins to abrogate at nanogram concentrations near 3.2 ng/mL (Figure 6). The diminishing of the signal at these concentrations is in agreement with doses at which the coefficient of friction begins to increase (Figure 1). Interestingly, the signal is only partially diminished and the molecular weight of lubricin appears to be lower at 0.1 $\mu\text{g}/\text{mL}$ (Figure 6). The diminishing of the ~460 kDa band corresponding to recombinant lubricin is lost at the same concentrations of StcE (3 ng/mL and above) in partially purified, recombinant lubricin, verifying the results for unpurified lubricin in SF. Immunodetection confirms the specific degradation of lubricin and validates the frictional data to effectively characterize lubrication modes for cartilage in lubricin-deficient SF.

DISCUSSION

The objective of the study was to evaluate and quantify the effect of StcE enzymatic treatment on SF lubrication. StcE was an extremely potent and effective enzyme, capable of significantly increasing the coefficients of friction in otherwise healthy BSF even at nanogram doses. On the Stribeck curve, high-friction PBS and low-friction BSF control measurements were consistent with previously published data for these models.⁴⁵ The trypsin and hyaluronidase treatments also yielded friction coefficients consistent with previous literature.²⁵ Notably, the relationship between the StcE and the measured coefficient of friction was dose-dependent. While

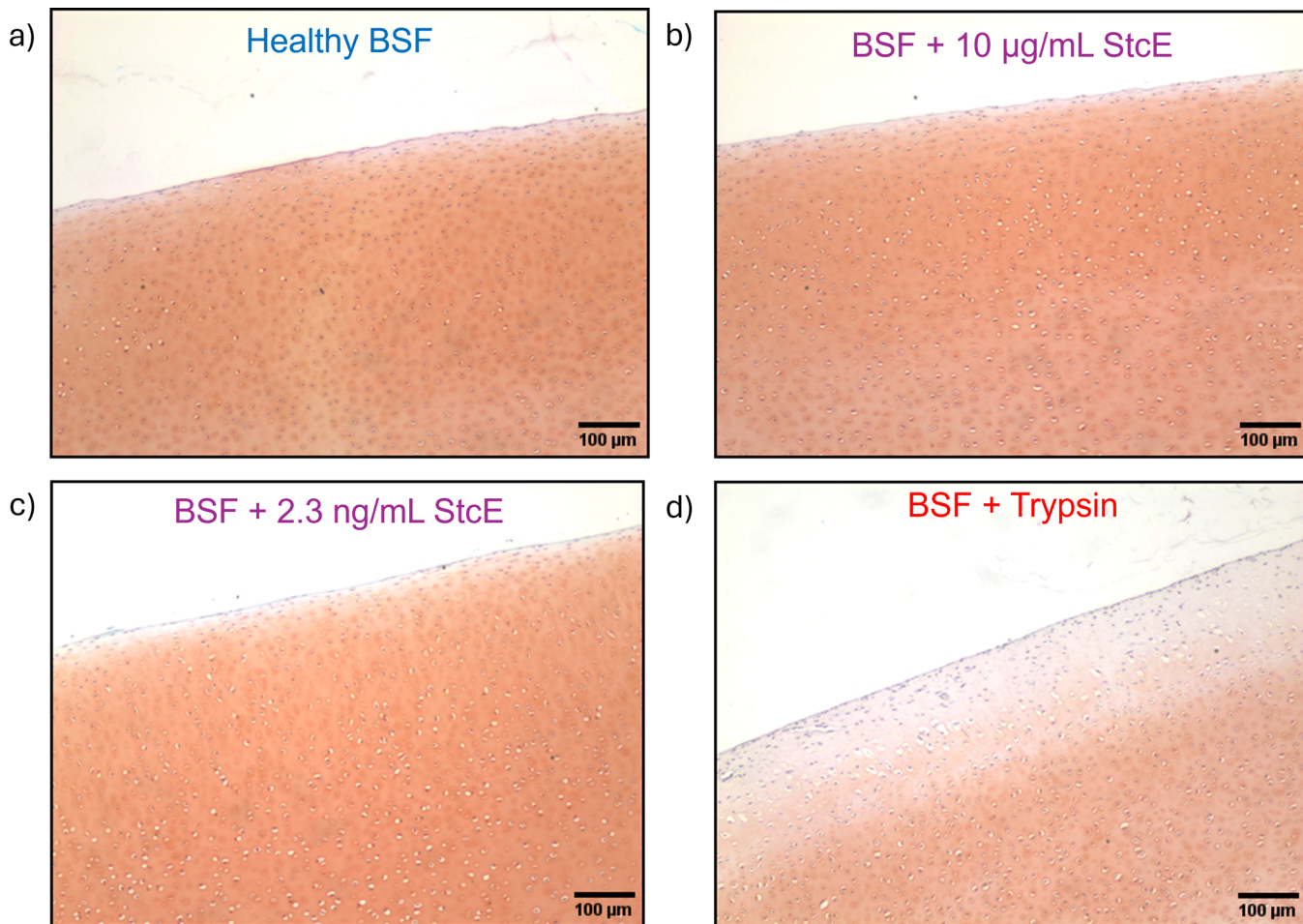


Figure 4. Safranin-O/Fast Green-stained histological sections of cartilage explants from (A) healthy BSF, (B–C) two doses of StcE at different orders of magnitude and (D) trypsin-treated BSF after friction test reveal that StcE treatments across all doses exhibit minimal structural changes or GAG depletion. Healthy BSF is consistent with previously observed morphology. As expected, the trypsin treatment fibrillates the cartilage surface and depletes GAG. Representative images presented for $n = 8$ per treatment. Scale bar = 100 μ m.

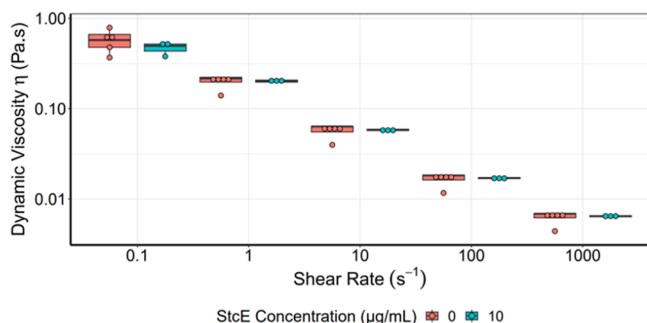


Figure 5. Dynamic viscosity measurements across 5 orders of magnitude of shear rate for healthy synovial fluid and StcE-treated synovial fluid show no significant differences in dynamic viscosity between the groups.

there were no observable visual trends in the Stribeck pattern across StcE groups (Figure 1), there was a clear difference in magnitude of the coefficients of friction across treatment groups. Increases to the coefficients of friction were observed at StcE treatments greater than 0.32 ng/mL, with the highest coefficients of friction at 10 ng/mL of StcE. Collectively, the verification of lubricin degradation by protein immunoblotting combined with the frictional and Stribeck trends in StcE treated synovial fluid demonstrate the specific role of lubricin

degradation in altering SF lubrication. While the loss of lubrication due to removal of lubricin's mucin domain was not entirely unexpected, the extent and specific nature of the frictional changes in SF lubrication provide valuable insights into the mechanisms of lubrication. Particularly, the dose-dependent nature of StcE highlights its ability to probe intermediate conditions representative of early stages of disease with partly truncated lubricin that may alter the uniform localization of a lubricin-HA layer, especially considering the recently discovered role of truncated lubricin on the inflammatory cytokine response.⁵⁶ The Stribeck model informs how the transition from the boundary lubrication regime to an elastoviscous mode occurs. Loss of SF lubrication is generally considered to be one of the early factors that accelerates the progression of OA leading to further physiological changes like articular cartilage degradation.⁹ This novel mucinase treatment provides a domain-specific enzyme that selectively cleaves the mucin domain, enabling the assessment of molecular mechanisms of cartilage lubrication (and providing insight into OA pathophysiology).

The ability to specifically target the mucin domain of lubricin enables for a more precise assessment of the contributions of individual proteins to SF lubrication. Previous work shows that although SF is composed largely of albumin and globulin, the comparably marginal concentrations of HA

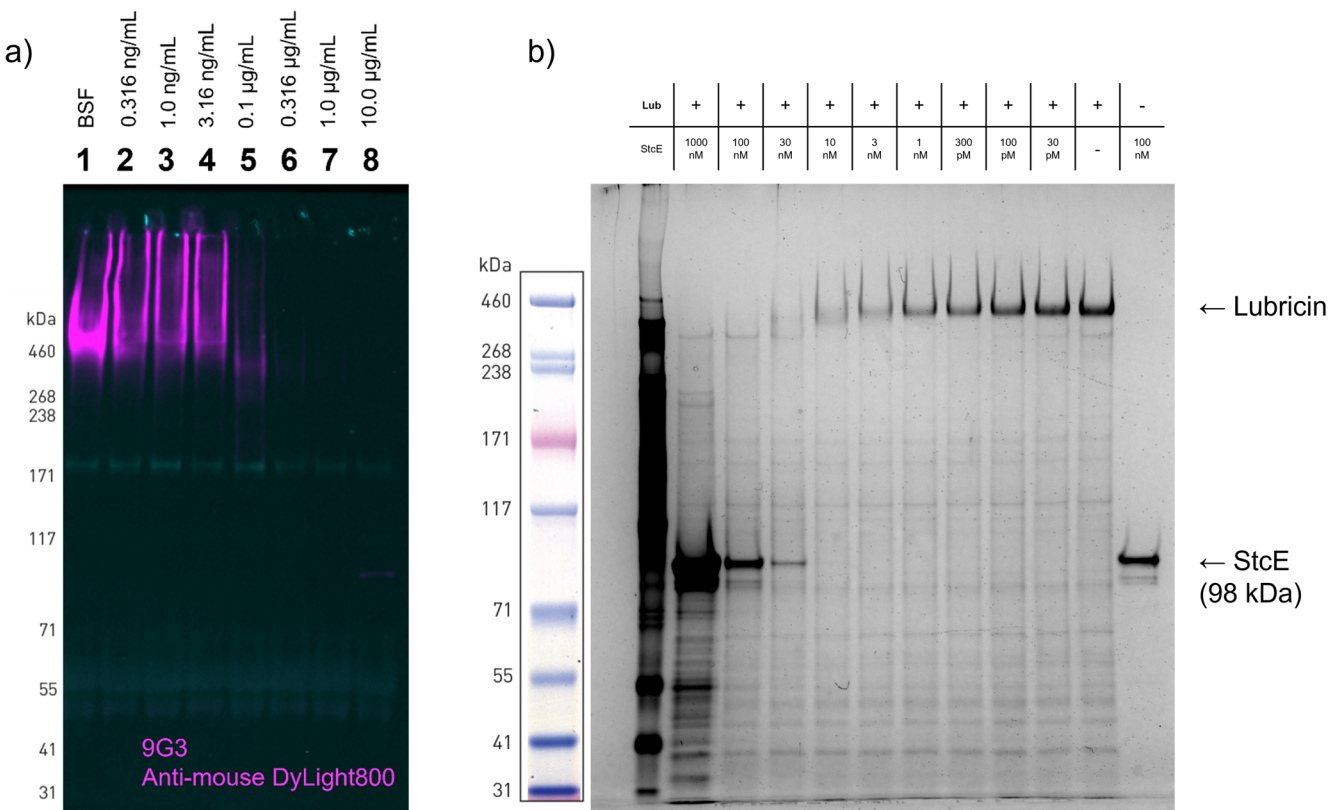


Figure 6. Immunoblotting of synovial fluid after friction testing with 9G3 Antilubricin monoclonal antibody and Antimouse DyLight800 secondary antibody reveal abrogation of the mucin domain signal at nanogram StcE concentrations for unpurified lubricin in SF (a). The signal begins diminishing at 3.16 ng/mL (column 4) and is completely abrogated at 0.316 µg/mL (column 6). Immunoblotting with partially purified, recombinant lubricin analyzed by SDS-PAGE and silver staining reveal that the major band at ~460 kDa corresponding to recombinant lubricin is lost following digestion with StcE at 3 ng/mL and above (b), consistent with results for unpurified lubricin in SF.

and lubricin in SF have substantial contributions to its lubrication.^{5,57} While it is known that pathological SF exhibits changes in the composition of these macromolecules, the extent to which the background globular proteins affect lubrication was unknown. While some studies involving enzymatic treatment of SF have previously used trypsin to assess the lubricating ability of lubricin, trypsin is known to have a degrading effect on other major proteins in SF as well.^{25,29,31,58} Notably, comparable friction values were observed between the trypsin group, where the majority of the protein component in SF is degraded, and the maximum effective StcE concentration group, where only the mucin domain of lubricin is fully degraded. Importantly, these data suggest that truncation of the O-glycosylated domain in lubricin is sufficient in significantly inhibiting the lubrication mechanism of SF, on par with SF with a completely degraded protein component.

Several studies have shown that the synergistic interactions between lubricin and HA are responsible for the low coefficients of friction of cartilage.^{17,19,21,25,59,60} This interaction likely prevents wear by forming a viscous gel-layer at the surface that is possibly several orders of magnitude more viscous than away from the surface in the bulk. The friction and Stribeck data substantiate these gel-layer theories and support the idea that nonspecific entanglement of HA to the mucin domains in lubricin drives this mechanism. Importantly, while previous studies analyzing scale-dependent rheology on steel cone-on-plate geometries have found a lack of interaction between HA and lubricin, rheological measurements on steel

geometries may not fully capture the complexity of glycosylation, protein and molecular interactions that occur in the joint environment.^{49,61} The experimental framework in this study reconciles these differences in *in vivo* and *ex-vivo* findings by simulating physiological conditions with high normal and shear stresses. Thus, the role of O-linked oligosaccharides on lubricin's mucin domain can be attributed to driving the formation of the gel-layer and providing hydration. The dose-dependent response of StcE treatment on the friction is concomitant with this observation, in which the presence of fewer O-glycosylated proteins disrupts the formation of the complex and no longer provides lubrication.

Further, the known mode of action of StcE by random cleavage of O-GalNAc sites implicates variable truncation of lubricin's mucin domain.³⁵ The variable length of the glycosylated domain across lubricin molecules may affect the uniformity of HA and lubricin localization at the surface to reduce friction.²⁰ While lubricin's N-terminus anchors lubricin to the cartilage surface at the contact point, the C-terminus facilitates higher-order aggregation of lubricin molecules by disulfide bond dimerization. The combined effect of the N- and C- terminus creates a uniform coat of localized, fully extended monomers and dimers that sterically repel adherent lubricin layers on apposing surfaces to reduce friction.²⁰ Truncation of lubricin likely disrupts lubricin dimerization and alters the distribution of lubricin across the cartilage surface, which may contribute to the inability to form a consistent lubricating layer as aforementioned.^{62,63}

The Stribeck framework provides additional insight into the role of lubricin in the speed dependence of cartilage friction. The Stribeck-like surface plot serves a 2-fold purpose, first enabling the characterization of lubrication modes in SF across different speeds and StcE doses, and then revealing speed-dependent friction trends at critical doses. Previous work suggests that lubricin mediates the shifts in friction to the boundary regime.²⁵ Consequently, lubricin digestion has been shown to disrupt the synergy between lubricin and HA and shifts the low friction behavior of these solutions from the elastoviscous friction regime back toward the boundary mode plateau. The results presented here indicate that the Stribeck surface for StcE treated BSF transitions from boundary mode to hydrodynamic mode as O-glycosylation increases. Notably, speed dependence is greatest at the ED₅₀ of StcE. At this intermediate concentration, the partial presence of O-glycosylated proteins in the environment would only be conducive to the formation of a friction reducing gel-layer at higher articulation speeds when contact stresses are minimized. As higher StcE doses reduces the presence of O-glycosylated proteins, it is possible that the gel-layer does not form regardless of articulation speed, which is reflected in the shift to the boundary lubrication mode at high friction coefficients. Conversely, StcE doses significantly below the ED₅₀ maintain their lubricating properties implicating the presence of lubricin-HA synergy. Thus, determining conditions in which the gel complex forms provide critical information on which endogenous environments may be more susceptible to changes in O-glycosylation and thus an osteoarthritic environment.

The friction coefficients of the StcE treatment were reported to be between $\mu = 0.09$ and 0.24 . The histological changes to the explants from PBS-lubricated and trypsin-treated BSF are consistent with previously reported data.⁵² Further, immuno-detection methods using a mucin domain-specific antilubricin monoclonal antibody confirmed the degradation of lubricin in SF. Importantly, the abrogation of this signal began at the same StcE concentrations that increased friction in the tribology experiments (~ 3.2 ng/mL), supporting the effectiveness of StcE in disrupting lubrication mechanisms in SF by mucin domain degradation. Additionally, a qualitative histological evaluation of the cartilage structure in the treatment groups after friction testing sufficiently supported the specificity of StcE. The visible depletion of glycosaminoglycans observed in the trypsin group is largely attributed to the trypsin induced cleavage of core proteoglycans on the surface of the cartilage sample bathed in treated SF. GAG depletion compromises lubricating ability and increases coefficient of friction, consistent with our findings. Because the StcE treatment group revealed no damage to cartilage structure or integrity, it supports the idea that high friction in StcE treatment is the result of StcE activity on lubricin. Additionally, rheological measurements reveal no significant differences in the viscosity of StcE at the highest dose of 10 μ g/mL, confirming that differences in HA composition in StcE treated BSF at the various compositions are minimal. These outcomes in friction, immunoblotting and histology bolster the reliability and robustness of the StcE mucinase treatment in degrading the lubricating ability of SF.

Loss of HA and lubricin localization and subsequent increased friction contributes to cartilage wear and OA development and progression.¹⁶ Truncated lubricin in SF is indicated as a joint disease biomarker known for exacerbating cytokine response and synovial inflammation and may also

affect friction.⁵⁶ Altered molecular compositions of lubricin, HA, and other proteins in the synovial fluid are used as key diagnostic markers for diseased or inflamed joints.¹³ Notably, changes in lubricin and HA concentrations persist over extended periods of time following joint disease initiation.⁹ As such, these macromolecules have been targets for joint therapy in intra-articular injections for many years and some studies have demonstrated the disease-modifying capabilities of lubricin injections in animal models.^{64–66} The novel tool and experimental framework presented in this study provides unique insights into the mechanisms underlying these therapeutic interventions. First, the data affirms that the O-linked oligosaccharide domains in lubricin primarily enhance cartilage lubrication. This points to the clinical importance of studying the regulation of lubricin glycosylation to more fully understand the pathogenesis of osteoarthritis. The high variability in the O-glycosylation patterns of lubricin's mucin domain and the impact of this variability on friction can further inform the findings of this study. New methods of genome editing combined with mammalian cell production platforms allow for the manufacturing of lubricin with highly customizable and tunable O-glycan structures. Future comparative friction studies for recombinant lubricin groups that vary in O-glycan density, length, and branch complexity could better inform the preferred structural characteristics of pre-existing lubricin-based therapies. Additionally, intermediate doses of StcE could be representative of some of the pathological changes observed in synovial fluid with the progression of disease or inflammation. At these doses, greater articulation speeds exhibited low-friction elastoviscous conditions while lower speeds transitioned otherwise healthy BSF to the high friction boundary mode. Since articular cartilage experiences a wide range of articulation speeds, high velocity and low load conditions occur during the unloaded swing phase of gait at which point intermediate lubricin concentrations would be capable of lubricating the joint while low velocity, high load conditions that occur during foot strike would not.^{67–69}

Another point of discussion is the effect of StcE on residual lubricin on the bathed cartilage samples. While it is possible that StcE in solution cleaves residual lubricin on the cartilage surface, the extent to which that residual lubricin lubricates cartilage is unknown and it is possible that the concentration of residual lubricin is well below the ED₅₀ for efficacious lubrication. Previous studies probing the frictional effects of endogenous lubricin have revealed relatively small changes in coefficient of friction between lubricin-extracted and non-extracted cartilage in SF compared to the frictional changes observed in this study.⁷⁰ Further, minimal fibrillation or damage to the cartilage surface was observed in nearly all histological sections and StcE in PBS showed minimal differences in friction from a PBS solution. Future IHC studies may provide valuable quantitative information on the spatial distribution of the degraded mucin domain within the cartilage tissue.

While this study effectively characterizes the lubricating ability of StcE-treated SF, there are some limitations to be discussed. Tribological methods in this study utilized cartilage explants from neonatal bovine femoral condyles. While this cartilage is not completely structurally representative of humans, it has been previously used in studies involving healthy and enzymatically treated articular cartilage.¹⁵ Furthermore, the friction coefficients in neonatal bovine cartilage have previously been shown to be predictive of

human cartilage systems.⁴⁷ Similar to the cartilage model, bovine synovial fluid was used for analyses. While this is a limitation, bovine and human articulating joints exhibit similarities in OA pathology, anatomy, and lubrication mechanism.^{71,72} Additionally, the availability of BSF coupled with the challenges that come with obtaining truly healthy human SF make BSF a desirable substitute. This study utilizes a stationary contact area configuration where the sliding counter face is polished glass. Previous studies have shown that cartilage-glass interfaces may deviate in their friction measurements from physiological cartilage-cartilage interfaces for specific molecules of interest like HA.⁷³ However, lubricin remains an effective lubricant in cartilage-glass systems and notably, polished glass counter faces bear boundary friction coefficients that are similar to those in cartilage-cartilage systems.⁶ Additionally, the presence of impurity bands in the lubricin and StcE samples make it difficult to identify the lubricin digest products with high confidence. Future methods of detection of purified lubricin digests with staining agents may further inform the valuable findings of this study by highlighting the impact of glycoform variability on cartilage lubrication. Lastly, the Stribeck framework traditionally maps friction as a function of Sommerfeld number, which is itself a function of normal load, sliding speed and viscosity. In this study, friction was only mapped as a function of sliding speed following rheology measurements in different StcE doses that confirmed no observable changes in the viscosity of the SF following treatment. Thus, while Sommerfeld number was not extensively used, a systematic evaluation of the contributing parameters to friction was still possible and provided a robust tool to study the lubricating mechanisms of articular cartilage in SF.

CONCLUSIONS

This study's application of a novel mucinase treatment successfully characterizes the pivotal role of the O-glycosylated domain in lubricin function, revealing dose-dependent modifications to SF lubrication. In doing so, it affirms that the gradual elimination of lubricin's mucin domain, which makes the environment conducive to HA surface aggregation causes a transition from an elastoviscous mode of lubrication to a high friction boundary mode. Fueled by recent advancements in glycobiology, these findings offer insights into the mucin-specific pathophysiological mechanisms underlying OA and open new frontiers for the development of biomimetic therapeutics aimed at mitigating the progression of OA.

ASSOCIATED CONTENT

Supporting Information

The Supporting Information is available free of charge at <https://pubs.acs.org/doi/10.1021/acsbiomaterials.4c00908>.

Includes comparative friction study between PBS and StcE treated-PBS for enzyme validity and friction data for all tested StcE doses ([PDF](#))

AUTHOR INFORMATION

Corresponding Author

Lawrence J. Bonassar — Meinig School of Biomedical Engineering, Cornell University, Ithaca, New York 14850, United States; Sibley School of Mechanical and Aerospace Engineering, Cornell University, Ithaca, New York 14850,

United States; [orcid.org/0000-0003-1094-6433](#); Phone: (607) 255-9381; Email: lb244@cornell.edu

Authors

Megh Prajapati — Meinig School of Biomedical Engineering, Cornell University, Ithaca, New York 14850, United States; [orcid.org/0009-0007-0155-2869](#)

Karan Vishwanath — Department of Materials Science and Engineering, Cornell University, Ithaca, New York 14853, United States

Lingting Huang — Robert Frederick Smith School of Chemical and Biomolecular Engineering, Cornell University, Ithaca, New York 14853, United States

Marshall Colville — Robert Frederick Smith School of Chemical and Biomolecular Engineering, Cornell University, Ithaca, New York 14853, United States; Dept. of Clinical Sciences, College of Veterinary Medicine, Cornell University, Ithaca, New York 14853, United States; [orcid.org/0000-0002-5397-8382](#)

Heidi Reesink — Dept. of Clinical Sciences, College of Veterinary Medicine, Cornell University, Ithaca, New York 14853, United States

Matthew Paszek — Robert Frederick Smith School of Chemical and Biomolecular Engineering, Cornell University, Ithaca, New York 14853, United States

Complete contact information is available at: <https://pubs.acs.org/10.1021/acsbiomaterials.4c00908>

Author Contributions

The manuscript was prepared through contributions of all authors. All authors have given approval of the final version of the manuscript. Megh Prajapati contributed to the research design, data acquisition, analysis, and interpretation as well as authoring and editing of this manuscript. Karan Vishwanath contributed to the research design, analysis and interpretation as well as authoring and editing of this manuscript. Lingting Huang contributed to the data acquisition and analysis of this manuscript. Marshall Colville contributed to the research design, data analysis and interpretation as well as editing of this manuscript. Heidi Reesink contributed to the data analysis and interpretation as well as editing of this manuscript. Matthew Paszek contributed to the data interpretation as well as editing of this manuscript. Lawrence J. Bonassar contributed to the research design, analysis, and interpretation as well as the authoring and editing of this manuscript.

Funding

This study was supported by the National Science Foundation LEAP-HI program under award number CMMI 2245367 and the Engineering Learning Initiatives (ELI) Undergraduate Research Student Grants Program in the College of Engineering at Cornell University.

Notes

The authors declare the following competing financial interest(s): Dr. Bonassar is a co-founder of and holds equity in 3DBio Corp and is a consultant for Fidia Farmaceutici, SpA and Histogenics, Inc.

ACKNOWLEDGMENTS

The authors would like to thank Serafina Lopez and Caroline Thompson for their technical assistance with histological staining and brightfield microscopic use. The authors would like to thank the Cornell College of Veterinary Medicine's

Animal Health Diagnostic Center for technical assistance in histological fixing and slide preparation.

■ ABBREVIATIONS

BSF, bovine synovial fluid; HA, hyaluronic acid; PRG4, proteoglycan 4; HAdase, hyaluronidase; GAG, glycosaminoglycan; IMAC, immobilized metal affinity chromatography; OA, osteoarthritis; SF, synovial fluid; StcE, secreted protease of C1 esterase inhibitor; VSCR, variable slope concentration response.

■ REFERENCES

- (1) Goldring, M. B. Articular Cartilage Degradation in Osteoarthritis. *HSS J.* **2012**, *8* (1), 7–9.
- (2) Sanchez-Lopez, E.; Coras, R.; Torres, A.; Lane, N. E.; Guma, M. Synovial Inflammation in Osteoarthritis Progression. *Nat. Rev. Rheumatol.* **2022**, *18* (5), 258–275.
- (3) Heinegård, D.; Saxne, T. The Role of the Cartilage Matrix in Osteoarthritis. *Nat. Rev. Rheumatol.* **2011**, *7* (1), 50–56.
- (4) Marian, M.; Shah, R.; Gashi, B.; Zhang, S.; Bhavnani, K.; Wartzack, S.; Rosenkranz, A. Exploring the Lubrication Mechanisms of Synovial Fluids for Joint Longevity - A Perspective. *Colloids Surf. B Biointerfaces* **2021**, *206*, No. 111926.
- (5) Ghosh, S.; Choudhury, D.; Das, N. S.; Pingguan-Murphy, B. Tribological Role of Synovial Fluid Compositions on Artificial Joints — a Systematic Review of the Last 10 Years. *Lubrication Science* **2014**, *26* (6), 387–410.
- (6) Schmidt, T. A.; Sah, R. L. Effect of Synovial Fluid on Boundary Lubrication of Articular Cartilage. *Osteoarthritis and Cartilage* **2007**, *15* (1), 35–47.
- (7) Schmidt, T. A.; Gastelum, N. S.; Nguyen, Q. T.; Schumacher, B. L.; Sah, R. L. Boundary Lubrication of Articular Cartilage: Role of Synovial Fluid Constituents. *Arthritis & Rheumatism* **2007**, *56* (3), 882–891.
- (8) Elsaïd, K. A.; Fleming, B. C.; Oksendahl, H. L.; Machan, J. T.; Fadale, P. D.; Hulstyn, M. J.; Shalvoy, R.; Jay, G. D. Decreased Lubricin Concentrations and Markers of Joint Inflammation in the Synovial Fluid of Patients with Anterior Cruciate Ligament Injury. *Arthritis & Rheumatism* **2008**, *58* (6), 1707–1715.
- (9) Feeney, E.; Peal, B. T.; Inglis, J. E.; Su, J.; Nixon, A. J.; Bonassar, L. J.; Reesink, H. L. Temporal Changes in Synovial Fluid Composition and Elastoviscous Lubrication in the Equine Carpal Fracture Model. *J. Orthop. Res.* **2019**, *37* (5), 1071–1079.
- (10) Antonacci, J. M.; Schmidt, T. A.; Serventi, L. A.; Cai, M. Z.; Shu, Y. L.; Schumacher, B. L.; McIlwraith, C. W.; Sah, R. L. Effects of Equine Joint Injury on Boundary Lubrication of Articular Cartilage by Synovial Fluid: Role of Hyaluronan. *Arthritis & Rheumatism* **2012**, *64* (9), 2917–2926.
- (11) Irwin, R. M.; Feeney, E.; Secchieri, C.; Galessio, D.; Cohen, I.; Oliviero, F.; Ramonda, R.; Bonassar, L. J. Distinct Tribological Endotypes of Pathological Human Synovial Fluid Reveal Characteristic Biomarkers and Variation in Efficacy of Viscosupplementation at Reducing Local Strains in Articular Cartilage. *Osteoarthritis Cartilage* **2020**, *28* (4), 492–501.
- (12) Buckwalter, J. A.; Mankin, H. J.; Grodzinsky, A. J. Articular Cartilage and Osteoarthritis. *Instr. Course Lect.* **2005**, *54*, 465–480.
- (13) Li, Y.; Yuan, Z.; Yang, H.; Zhong, H.; Peng, W.; Xie, R. Recent Advances in Understanding the Role of Cartilage Lubrication in Osteoarthritis. *Molecules* **2021**, *26* (20), 6122.
- (14) Cooke, M. E.; Lawless, B. M.; Jones, S. W.; Grover, L. M. Matrix Degradation in Osteoarthritis Primes the Superficial Region of Cartilage for Mechanical Damage. *Acta Biomaterialia* **2018**, *78*, 320–328.
- (15) Bonnevie, E. D.; Galessio, D.; Secchieri, C.; Bonassar, L. J. Degradation Alters the Lubrication of Articular Cartilage by High Viscosity, Hyaluronic Acid-Based Lubricants. *Journal of Orthopaedic Research* **2018**, *36* (5), 1456–1464.
- (16) Neu, C. P.; Reddi, A. H.; Komvopoulos, K.; Schmid, T. M.; Di Cesare, P. E. Increased Friction Coefficient and Superficial Zone Protein Expression in Patients with Advanced Osteoarthritis. *Arthritis Rheum.* **2010**, *62* (9), 2680–2687.
- (17) Das, S.; Banquy, X.; Zappone, B.; Greene, G. W.; Jay, G. D.; Israelachvili, J. N. Synergistic Interactions between Grafted Hyaluronic Acid and Lubricin Provide Enhanced Wear Protection and Lubrication. *Biomacromolecules* **2013**, *14* (5), 1669–1677.
- (18) Jay, G. D.; Torres, J. R.; Warman, M. L.; Laderer, M. C.; Breuer, K. S. The Role of Lubricin in the Mechanical Behavior of Synovial Fluid. *Proc. Natl. Acad. Sci. U. S. A.* **2007**, *104* (15), 6194–6199.
- (19) Ye, H.; Han, M.; Huang, R.; Schmidt, T. A.; Qi, W.; He, Z.; Martin, L. L.; Jay, G. D.; Su, R.; Greene, G. W. Interactions between Lubricin and Hyaluronic Acid Synergistically Enhance Antiadhesive Properties. *ACS Appl. Mater. Interfaces* **2019**, *11* (20), 18090–18102.
- (20) Jay, G. D.; Waller, K. A. The Biology of Lubricin: Near Frictionless Joint Motion. *Matrix Biol.* **2014**, *39*, 17–24.
- (21) Majd, S. E.; Kuijper, R.; Köwitsch, A.; Groth, T.; Schmidt, T. A.; Sharma, P. K. Both Hyaluronan and Collagen Type II Keep Proteoglycan 4 (Lubricin) at the Cartilage Surface in a Condition That Provides Low Friction during Boundary Lubrication. *Langmuir* **2014**, *30* (48), 14566–14572.
- (22) Jay, G. D.; Harris, D. A.; Cha, C. J. Boundary Lubrication by Lubricin Is Mediated by O-Linked Beta(1–3)Gal-GalNAc Oligosaccharides. *Glycoconj. J.* **2001**, *18* (10), 807–815.
- (23) Zappone, B.; Ruths, M.; Greene, G. W.; Jay, G. D.; Israelachvili, J. N. Adsorption, Lubrication, and Wear of Lubricin on Model Surfaces: Polymer Brush-Like Behavior of a Glycoprotein. *Biophys. J.* **2007**, *92* (5), 1693–1708.
- (24) Gleghorn, J. P.; Jones, A. R. C.; Flannery, C. R.; Bonassar, L. J. Boundary Mode Lubrication of Articular Cartilage by Recombinant Human Lubricin. *J. Orthop. Res.* **2009**, *27* (6), 771–777.
- (25) Bonnevie, E. D.; Galessio, D.; Secchieri, C.; Cohen, I.; Bonassar, L. J. Elastoviscous Transitions of Articular Cartilage Reveal a Mechanism of Synergy between Lubricin and Hyaluronic Acid. *PLoS One* **2015**, *10* (11), No. e0143415.
- (26) Lin, W.; Liu, Z.; Kampf, N.; Klein, J. The Role of Hyaluronic Acid in Cartilage Boundary Lubrication. *Cells* **2020**, *9* (7), 1606.
- (27) Szychlinska, M. A.; Leonardi, R.; Al-Qahtani, M.; Moshaveri, A.; Musumeci, G. Altered Joint Tribology in Osteoarthritis: Reduced Lubricin Synthesis Due to the Inflammatory Process. New Horizons for Therapeutic Approaches. *Ann. Phys. Rehabil. Med.* **2016**, *59* (3), 149–156.
- (28) Watkins, A. R.; Reesink, H. L. Lubricin in Experimental and Naturally Occurring Osteoarthritis: A Systematic Review. *Osteoarthritis and Cartilage* **2020**, *28* (10), 1303–1315.
- (29) Jay, G. D. Characterization of a Bovine Synovial Fluid Lubricating Factor. I. Chemical, Surface Activity and Lubricating Properties. *Connective Tissue Research* **1992**, *28* (1–2), 71–88.
- (30) Sun, Y.; Chen, M.-Y.; Zhao, C.; An, K.-N.; Amadio, P. C. The Effect of Hyaluronidase, Phospholipase, Lipid Solvent and Trypsin on the Lubrication of Canine Flexor Digitorum Profundus Tendon. *Journal of Orthopaedic Research* **2008**, *26* (9), 1225–1229.
- (31) Kempson, G. E.; Tuke, M. A.; Dingle, J. T.; Barrett, A. J.; Horsefield, P. H. The Effects of Proteolytic Enzymes on the Mechanical Properties of Adult Human Articular Cartilage. *Biochimica et Biophysica Acta (BBA) - General Subjects* **1976**, *428* (3), 741–760.
- (32) Moody, H. R.; Brown, C. P.; Bowden, J. C.; Crawford, R. W.; McElwain, D. L. S.; Oloyede, A. O. In Vitro Degradation of Articular Cartilage: Does Trypsin Treatment Produce Consistent Results? *Journal of Anatomy* **2006**, *209* (2), 259–267.
- (33) Harris, E. D.; Parker, H. G.; Radin, E. L.; Krane, S. M. Effects of Proteolytic Enzymes on Structural and Mechanical Properties of Cartilage. *Arthritis Rheum.* **1972**, *15* (5), 497–503.
- (34) Kesimer, M.; Sheehan, J. K. Mass Spectrometric Analysis of Mucin Core Proteins. In *Mucins: Methods and Protocols*; McGuckin, M. A., Thornton, D. J., Eds.; Humana Press: Totowa, NJ, 2012; pp 67–79. .

(35) Malaker, S. A.; Pedram, K.; Ferracane, M. J.; Bensing, B. A.; Krishnan, V.; Pett, C.; Yu, J.; Woods, E. C.; Kramer, J. R.; Westerlind, U.; Dorigo, O.; Bertozzi, C. R. The Mucin-Selective Protease StcE Enables Molecular and Functional Analysis of Human Cancer-Associated Mucins. *Proc. Natl. Acad. Sci. U. S. A.* **2019**, *116* (15), 7278–7287.

(36) Julenius, K.; Mølgaard, A.; Gupta, R.; Brunak, S. Prediction, Conservation Analysis, and Structural Characterization of Mammalian Mucin-Type O-Glycosylation Sites. *Glycobiology* **2005**, *15* (2), 153–164.

(37) Malaker, S. A.; Riley, N. M.; Shon, D. J.; Pedram, K.; Krishnan, V.; Dorigo, O.; Bertozzi, C. R. Revealing the Human Mucinome. *Nat. Commun.* **2022**, *13* (1), 3542.

(38) Ali, L.; Flowers, S. A.; Jin, C.; Bennet, E. P.; Ekwall, A.-K. H.; Karlsson, N. G. The O-Glycomap of Lubricin, a Novel Mucin Responsible for Joint Lubrication, Identified by Site-Specific Glycopeptide Analysis. *Mol. Cell Proteomics* **2014**, *13* (12), 3396–3409.

(39) Liu, C.; Madl, A. C.; Cirera-Salinas, D.; Kress, W.; Straube, F.; Myung, D.; Fuller, G. G. Mucin-Like Glycoproteins Modulate Interfacial Properties of a Mimetic Ocular Epithelial Surface. *Adv. Sci. (Weinh)* **2021**, *8* (16), No. e2100841.

(40) Shi, L.; Sikavitsas, V. I.; Striolo, A. Experimental Friction Coefficients for Bovine Cartilage Measured with a Pin-on-Disk Tribometer: Testing Configuration and Lubricant Effects. *Ann. Biomed Eng.* **2011**, *39* (1), 132–146.

(41) Gleghorn, J. P.; Bonassar, L. J. Lubrication Mode Analysis of Articular Cartilage Using Stribeck Surfaces. *J. Biomech.* **2008**, *41* (9), 1910–1918.

(42) Farnham, M. S.; Larson, R. E.; Burris, D. L.; Price, C. Effects of Mechanical Injury on the Tribological Rehydration and Lubrication of Articular Cartilage. *Journal of the Mechanical Behavior of Biomedical Materials* **2020**, *101*, No. 103422.

(43) Dunn, A. C.; Angelini, T. E.; Pruitt, J.; Sawyer, W. G. Gemini Interfaces in Aqueous Lubrication of Hydrogels. *Invest. Ophthalmol. Visual Sci.* **2014**, *55* (13), 4656.

(44) Hersey, M. D. The Laws of Lubrication of Horizontal Journal Bearings. *J. Washington Acad. Sci.* **1914**, *4* (19), 542–552.

(45) Vishwanath, K.; McClure, S. R.; Bonassar, L. J. Polyacrylamide Hydrogel Lubricates Cartilage after Biochemical Degradation and Mechanical Injury. *Journal of Orthopaedic Research* **2023**, *41* (1), 63–71.

(46) Chang, D. P.; Abu-Lail, N. I.; Guilak, F.; Jay, G. D.; Zauscher, S. Conformational Mechanics, Adsorption, and Normal Force Interactions of Lubricin and Hyaluronic Acid on Model Surfaces. *Langmuir* **2008**, *24* (4), 1183–1193.

(47) Bonnevie, E. D.; Galessio, D.; Secchieri, C.; Bonassar, L. J. Frictional Characterization of Injectable Hyaluronic Acids Is More Predictive of Clinical Outcomes than Traditional Rheological or Viscoelastic Characterization. *PLoS One* **2019**, *14* (5), No. e0216702.

(48) Burris, D. L.; Sawyer, W. G. Addressing Practical Challenges of Low Friction Coefficient Measurements. *Tribol. Lett.* **2009**, *35* (1), 17–23.

(49) Vishwanath, K.; Secor, E. J.; Watkins, A.; Reesink, H. L.; Bonassar, L. J. Loss of Effective Lubricating Viscosity Is the Primary Mechanical Marker of Joint Inflammation in Equine Synovitis. *J. Orthop. Res.* **2024**, *42*, 1438.

(50) Ai, M.; Cui, Y.; Sy, M.-S.; Lee, D. M.; Zhang, L. X.; Larson, K. M.; Kurek, K. C.; Jay, G. D.; Warman, M. L. Anti-Lubricin Monoclonal Antibodies Created Using Lubricin-Knockout Mice Immunodetect Lubricin in Several Species and in Patients with Healthy and Diseased Joints. *PLoS One* **2015**, *10* (2), No. e0116237.

(51) Davis, W. H.; Lee, S. L.; Sokoloff, L. Boundary Lubricating Ability of Synovial Fluid in Degenerative Joint Disease. *Arthritis Rheum.* **1978**, *21* (7), 754–756.

(52) Griffin, D. J.; Vicari, J.; Buckley, M. R.; Silverberg, J. L.; Cohen, I.; Bonassar, L. J. Effects of Enzymatic Treatments on the Depth-Dependent Viscoelastic Shear Properties of Articular Cartilage. *Journal of Orthopaedic Research* **2014**, *32* (12), 1652–1657.

(53) Martin-Alarcon, L.; Schmidt, T. A. Rheological Effects of Macromolecular Interactions in Synovial Fluid. *Biorheology* **2016**, *53*, 49–19.

(54) Ludwig, T. E.; Cowman, M. K.; Jay, G. D.; Schmidt, T. A. Effects of concentration and structure on proteoglycan 4 rheology and interaction with hyaluronan. *Biorheology* **2014**, *51*, 409–422.

(55) Zhang, Z.; Barman, S.; Christopher, G. F. The Role of Protein Content on the Steady and Oscillatory Shear Rheology of Model Synovial Fluids. *Soft Matter* **2014**, *10* (32), 5965–5973.

(56) Huang, S.; Thomsson, K. A.; Jin, C.; Ryberg, H.; Das, N.; Struglics, A.; Rolfson, O.; Björkman, L. I.; Eisler, T.; Schmidt, T. A.; Jay, G. D.; Krawetz, R.; Karlsson, N. G. Truncated Lubricin Glycans in Osteoarthritis Stimulate the Synoviocyte Secretion of VEGFA, IL-8, and MIP-1 α : Interplay between O-Linked Glycosylation and Inflammatory Cytokines. *Front. Mol. Biosci.* **2022**, *9*, No. 942406.

(57) Furmann, D.; Něcas, D.; Rebenda, D.; Čípek, P.; Vrbka, M.; Křupka, I.; Hartl, M. The Effect of Synovial Fluid Composition, Speed and Load on Frictional Behaviour of Articular Cartilage. *Materials* **2020**, *13* (6), 1334.

(58) Chan, S. M. T.; Neu, C. P.; DuRaine, G.; Komvopoulos, K.; Reddi, A. H. Atomic Force Microscope Investigation of the Boundary-Lubricant Layer in Articular Cartilage. *Osteoarthritis and Cartilage* **2010**, *18* (7), 956–963.

(59) Huang, J.; Qiu, X.; Xie, L.; Jay, G. D.; Schmidt, T. A.; Zeng, H. Probing the Molecular Interactions and Lubrication Mechanisms of Purified Full-Length Recombinant Human Proteoglycan 4 (rhPRG4) and Hyaluronic Acid (HA). *Biomacromolecules* **2019**, *20* (2), 1056–1067.

(60) Ludwig, T. E.; Hunter, M. M.; Schmidt, T. A. Cartilage Boundary Lubrication Synergism Is Mediated by Hyaluronan Concentration and PRG4 Concentration and Structure. *BMC Musculoskelet Disord* **2015**, *16* (1), 386.

(61) Martin-Alarcon, L.; Govedarica, A.; Ewoldt, R. H.; Bryant, S. L.; Jay, G. D.; Schmidt, T. A.; Trifkovic, M. Scale-Dependent Rheology of Synovial Fluid Lubricating Macromolecules. *Small* **2024**, *20* (21), 2306207.

(62) Das, N.; de Almeida, L. G. N.; Derakhshani, A.; Young, D.; Mehdinejadani, K.; Salo, P.; Rezansoff, A.; Jay, G. D.; Sommerhoff, C. P.; Schmidt, T. A.; Krawetz, R.; Dufour, A. Tryptase β Regulation of Joint Lubrication and Inflammation via Proteoglycan-4 in Osteoarthritis. *Nat. Commun.* **2023**, *14* (1), 1910.

(63) Regmi, S. C.; Samsom, M. L.; Heynen, M. L.; Jay, G. D.; Sullivan, B. D.; Srinivasan, S.; Caffery, B.; Jones, L.; Schmidt, T. A. Degradation of Proteoglycan 4/Lubricin by Cathepsin S: Potential Mechanism for Diminished Ocular Surface Lubrication in Sjögren's Syndrome. *Exp. Eye Res.* **2017**, *161*, 1–9.

(64) Jay, G. D.; Fleming, B. C.; Watkins, B. A.; McHugh, K. A.; Anderson, S. C.; Zhang, L. X.; Teeple, E.; Waller, K. A.; Elsaid, K. A. Prevention of Cartilage Degeneration and Restoration of Chondroprotection by Lubricin Tribosupplementation in the Rat Following Anterior Cruciate Ligament Transection. *Arthritis Rheum.* **2010**, *62* (8), 2382–2391.

(65) Bao, J.-P.; Chen, W.-P.; Wu, L.-D. Lubricin: A Novel Potential Biotherapeutic Approaches for the Treatment of Osteoarthritis. *Mol. Biol. Rep.* **2011**, *38* (5), 2879–2885.

(66) Teeple, E.; Elsaid, K. A.; Jay, G. D.; Zhang, L.; Badger, G. J.; Akelman, M.; Bliss, T. F.; Fleming, B. C. Effects of Supplemental Intra-Articular Lubricin and Hyaluronic Acid on the Progression of Posttraumatic Arthritis in the Anterior Cruciate Ligament-Deficient Rat Knee. *Am. J. Sports Med.* **2011**, *39* (1), 164–172.

(67) Elsaid, K. A.; Jay, G. D.; Warman, M. L.; Rhee, D. K.; Chichester, C. O. Association of Articular Cartilage Degradation and Loss of Boundary-Lubricating Ability of Synovial Fluid Following Injury and Inflammatory Arthritis. *Arthritis Rheum.* **2005**, *52* (6), 1746–1755.

(68) Balazs, E. A.; Watson, D.; Duff, I. F.; Roseman, S. Hyaluronic Acid in Synovial Fluid. I. Molecular Parameters of Hyaluronic Acid in Normal and Arthritis Human Fluids. *Arthritis Rheum.* **1967**, *10* (4), 357–376.

(69) Ragan, C.; Meyer, K. THE HYALURONIC ACID OF SYNOVIAL FLUID IN RHEUMATOID ARTHRITIS. *J. Clin Invest* **1949**, *28* (1), 56–59.

(70) Gleghorn, J. P.; Jones, A. R. C.; Flannery, C. R.; Bonassar, L. J. Boundary Mode Lubrication of Articular Cartilage by Recombinant Human Lubricin. *Journal of Orthopaedic Research* **2009**, *27* (6), 771–777.

(71) Jay, G. D.; Haberstroh, K.; Cha, C.-J. Comparison of the Boundary-Lubricating Ability of Bovine Synovial Fluid, Lubricin, and Healon. *J. Biomed. Mater. Res.* **1998**, *40* (3), 414–418.

(72) Swann, D. A.; Silver, F. H.; Slayter, H. S.; Stafford, W.; Shore, E. The Molecular Structure and Lubricating Activity of Lubricin Isolated from Bovine and Human Synovial Fluids. *Biochem. J.* **1985**, *225* (1), 195–201.

(73) Abubacker, S.; McPeak, A.; Dorosz, S. G.; Egberts, P.; Schmidt, T. A. Effect of Counterface on Cartilage Boundary Lubricating Ability by Proteoglycan 4 and Hyaluronan: Cartilage-Glass versus Cartilage-Cartilage. *J. Orthop. Res.* **2018**, *36* (11), 2923–2931.